Optical analysis of HRR field

F. P. Chiang, MEMBER SPIE
T. V. Hareesh
B. C. Liu
S. Li
State University of New York at Stony Brook
Laboratory for Experimental Mechanics Research
Stony Brook, New York 11794-2300

Abstract. This paper examines the experimental u_1, u_2, and u_3 displacements obtained in the vicinity of a plastically deformed crack tip in different work hardening materials in the background of the Hutchinson-Rice-Rosengren (HRR) field equations. It is shown that the two-dimensional plane stress solution breaks down in the immediate vicinity of the crack tip because of the three-dimensional nature of the deformations due to finite plate thickness. This "inner limit" seems to vary from 0.75 to 1.5 times the thickness with directional dependence. Some light is also shed on the "outer limit" of HRR equations, beyond which the theory ceases to be valid under the influence of the surrounding elastic field or the physical boundary of the plate or a combination of both.

Subject terms: photomechanics; moire methods; elastic-plastic fracture; work hardening; three-dimensional deformations.

Optical Engineering 27(8), 625-629 (August 1988).

CONTENTS

1. INTRODUCTION

Lately there has been considerable interest in experimentally investigating the nature of the prevailing displacement, strain, and stress fields in the vicinity of a deformed crack tip. More often than not, the crack tip fields are described by Westergaard's equations under elastic or small scale yielding conditions and by the Hutchinson-Rice-Rosengren (HRR) equations[1,2] when yielding is significant and comparable to the uncracked specimen length. These are simple plane stress or plane strain models based on classical 2-D assumptions. However, in practice, one often uses materials with finite thickness that are approximated to either plane stress or plane strain conditions. It is well known that the existing field near the deforming crack tip is highly complex and three-dimensional. This results in the breakdown of 2-D assumptions in a region close to the crack tip. Rosakis and Ravi Chandar[3] investigated these 3-D effects using the method of caustics in elastic situations. They observed that plane stress assumptions are valid beyond about one-half of the plate thickness. Chiang and Hareesh[4] have used a combined moire method to study deformation fields near a plastically deformed crack tip in a low hardening aluminum. Results suggest that there is a zone of 3-D effects around the crack tip that could vary from 0.75 to 1.5 times the plate thickness with directional dependence. Recently, Zehnder et al.[5] have used the method of reflection caustics and finite elements to imply that HRR field equations under plane stress conditions have an outer limit of validity. Their results show that this limit seems to occur at about a third of Irwin's plastic zone length factor. Kang et al.[6,7] have also observed, in their displacement fields obtained from white light interferometry, that the HRR field prevails near the crack tip. Numerical calculations performed by Shih[8] show that J-dominance in plane strain conditions prevails over short distances of 1% to 7% of the uncracked ligament length, depending upon whether the crack is under pure tension or pure bending. It is anticipated to prevail over longer lengths when the crack is under plane stress.*

In this study we further investigate the inner (3-D zone) and outer limits of HRR displacement and strain descriptions in single edge notch (SEN) samples of materials with various hardening indices. The sample geometry chosen is such that the material could globally be assumed to be under plane stress loading.

2. EXPERIMENTAL TECHNIQUE

A combined in-plane and out-of-plane moire method[4] is used in this study to simultaneously obtain all three components of displacement u_1, u_2, and u_3 along the x_1, x_2, and x_3 directions, respectively. The experimental arrangement is shown in Fig. 1(a), and the specimen geometry is shown in Fig. 1(b). To begin

Invited Paper PH-105 received June 10, 1987; revised manuscript received May 27, 1988; accepted for publication May 27, 1988; received by Managing Editor May 31, 1988. This paper is a revision of Paper 814-90, presented at the SPIE International Conference on Photomechanics and Speckle Metrology, Aug. 17–20, 1987, San Diego, Calif. The paper presented there appears (unrefereed) in SPIE Proceedings Vol. 814, Part Two.

*C. F. Shih, private communications, 1987.

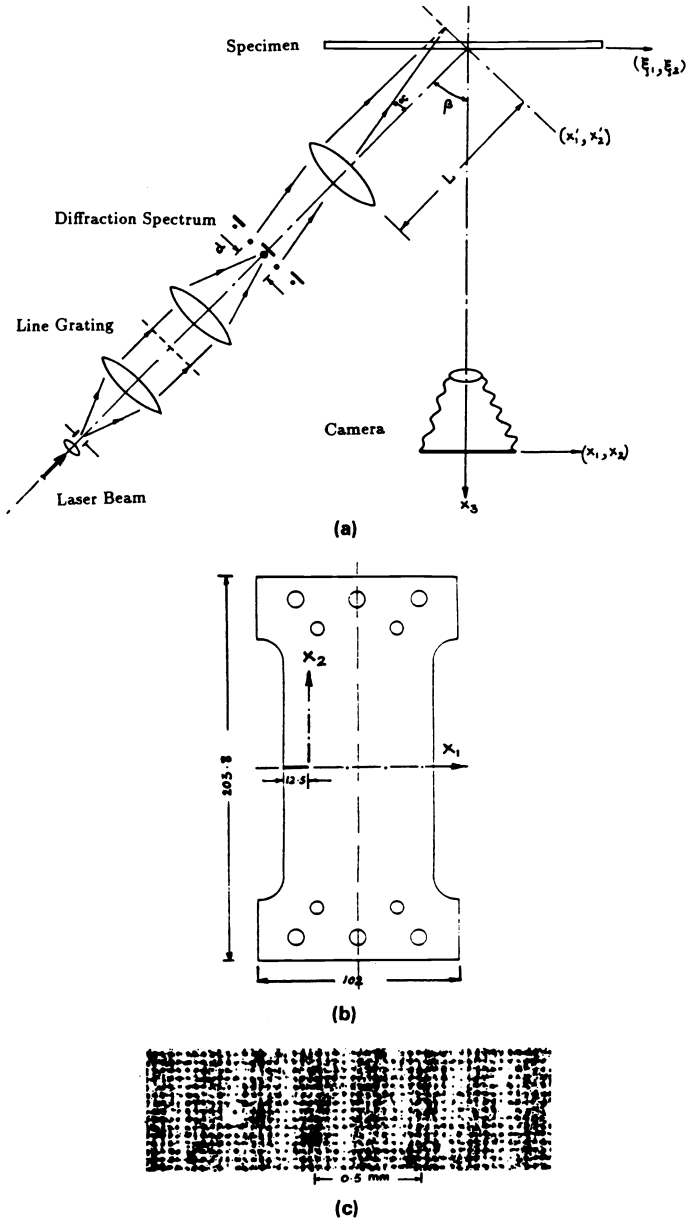

Fig. 1. (a) Experimental setup. (b) Specimen geometry (dimensions in millimeters). (c) Enlarged recorded grating.

with, the SEN specimen is printed with a cross grating of pitch p using a photoengraving process. Typical values of p in this study are 50.8 μm and 25.4 μm.

A He-Ne laser beam is first expanded by a microscope objective and then collimated by a field lens before it impinges upon a line grating. The regular and diffracted wavefronts are collected by a second field lens, which forms the diffraction spectrum of the grating at its focal plane in the form of a series of equally spaced bright dots called diffraction orders. All the orders are blocked by a mask except the ±1 orders, which are collected by a third lens to form two nearly collimated beams with an angle 2α between them to impinge upon the specimen. Within the intersecting beams there exists a standing wave of period (or pitch)

$$q' = \frac{\lambda}{2\sin\alpha} \quad , \tag{1}$$

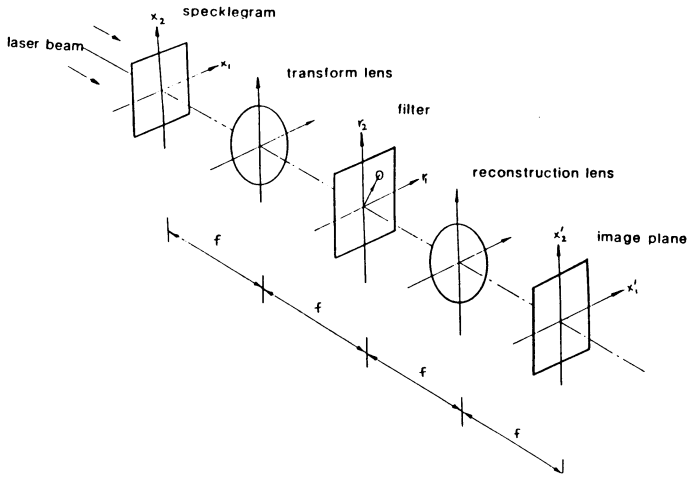

Fig. 2. Schematic for optical spatial filtering.

where λ is the wavelength.

When a specimen is placed in this field, it is covered by two patterns. One is the projected grating from the standing wave with a pitch

$$q = \frac{\lambda}{2\sin\alpha\cos\beta} \quad , \tag{2}$$

where β is the angle between the normal to the plate and the optical axis of the projection system. Another is the photographically printed pattern on the specimen surface. This entire optical field on the specimen is recorded before load is applied (master grating) and after load is applied (deformed grating). Several deformed gratings are recorded, corresponding to different load levels. An enlargement of one such recording is shown in Fig. 1(c). Each of the deformed gratings contains the information corresponding to all three displacement components. All these can be delineated in the form of contour fringes of displacement component through a process called optical spatial filtering.[9] A system for performing filtering is shown schematically in Fig. 2. A superimposed pair of master grating and deformed grating is placed in a coherent light field to display the spatial frequency content of the recordings at the Fourier transform plane of the first field lens. By appropriately selecting the diffraction order at this plane to be collected by the second lens, one can obtain contour fringes of u_1, u_2, and u_3. Their governing equations are

$$u_1 = Np \quad , \tag{3}$$

$$u_2 = N'p \quad , \tag{4}$$

$$u_3 = \frac{N''\lambda}{4\tan\alpha\sin\beta} \quad , \tag{5}$$

where N, N′, and N″ = 0, ±1, ±2, ±3, etc.

3. EXPERIMENTS

Three aluminum alloys of different hardening indices (n) were used in this study: Al2024-0 (n ≈ 3), Al5052-H32 (n ≈ 7), and Al6061-T6 (n ≈ 18). We calibrated the materials by using a simple tension test and fitting a Ramberg-Osgood type of curve, i.e.,

$$\frac{\varepsilon}{\varepsilon_o} = \frac{\sigma}{\sigma_o} + \alpha \left(\frac{\sigma}{\sigma_o}\right)^n \quad , \tag{6}$$

to the data points. In the above equation, σ_o is the yield stress, ε_o is the yield strain, n is the hardening index, and α is a material constant.

SEN samples were made from 3.17 mm thick sheets with rolling direction parallel to the loading axis of the specimen. Initially, notches 12 mm long were cut into each specimen by the electrodischarge machining (EDM) process. Fatigue cracks were grown in these EDM samples by subjecting them to sinusoidal tensile-to-tensile cyclic loads. The cyclic load levels were kept to a small fraction of the yield stress (typically 30% of σ_o), and notches were extended to about 14.5 mm. These samples were then subjected to monotonically increasing load, and deformed gratings were recorded at different load levels. The filtering process mentioned in the previous section resulted in the typical fringe patterns shown in Fig. 3. Here all three displacement contours are shown for the three materials chosen at the indicated load levels. Each fringe represents a displacement value of one pitch.

4. EXPERIMENTAL RESULTS COMPARED TO HRR EQUATIONS

HRR singularity descriptions[1,2] are widely accepted and used in the study of plastically deformed cracks in work hardening materials. The dominant strain-stress relationship based on deformation theory of plasticity for a hardening material is given by

$$\varepsilon_{ij} = \frac{3}{2}\alpha\sigma_e^{n-1}\frac{s_{ij}}{E} \quad , \tag{7}$$

where E is Young's modulus and s_{ij} is the stress deviator of σ_{ij}. Here σ_e is the effective stress given by $\sigma_e = \sqrt{(3/2)(s_{ij}s_{ij})}$. Using the stress function approach, Hutchinson, Rice, and Rosengren derived plane stress field equations for strain and displacement components as

$$\varepsilon_{ij}(r, \theta) = \alpha\varepsilon_o C^{n/(n+1)}\hat{\varepsilon}_{ij}(\theta, n) \quad , \tag{8}$$

$$u_i(r, \theta) = \alpha\varepsilon_o r C^{n/(n+1)}\hat{u}_i(\theta, n) \quad , \tag{9}$$

where

$$C = \frac{J}{\alpha\sigma_o\varepsilon_o I_n r} \quad .$$

Under plane stress conditions, the out-of-plane displacement u_3 can be expressed in terms of average u_3 direction strain:

$$\varepsilon_{33}^p \approx -\frac{2u_3}{h} = -(\varepsilon_{rr}^p + \varepsilon_{\theta\theta}^p) \quad , \tag{10}$$

where h is the thickness of the undeformed sheet. In the above equations, J is Rice's path-independent contour integral around the crack tip, given by

$$J = \int_\Gamma W dx_2 - \sigma_{ij} n_j u_{i,x_1} ds \quad ,$$

where Γ is the path of integration,

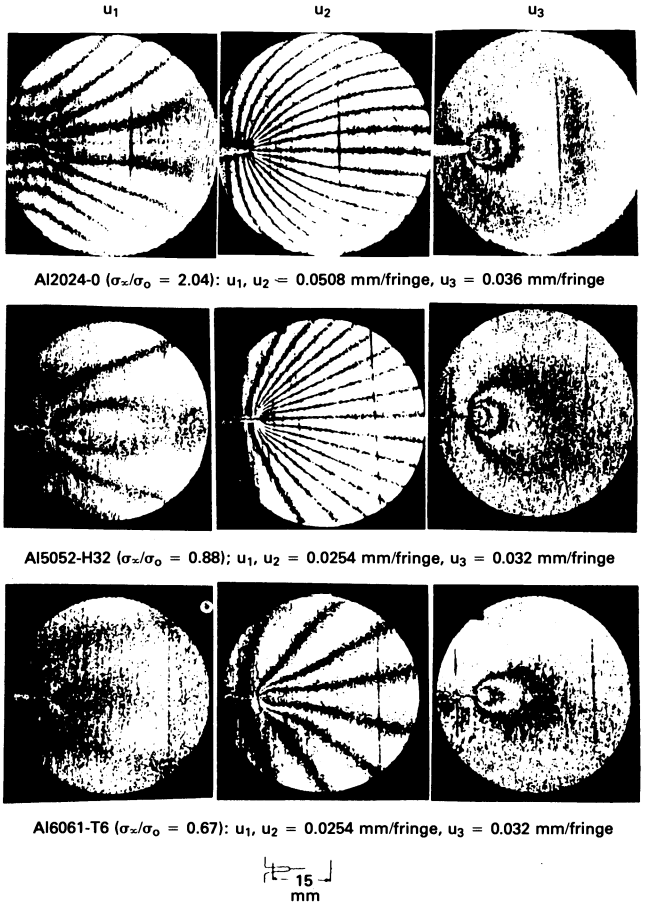

Material	σ_o kg/mm²	ε_o	α	n
Al 2024-0	5.0	0.00067	1.9	3.05
Al 5052-H32	17.0	0.0023	3.75	7.3
Al 6061-T6	28.0	0.004	1.22	18.0

Fig. 3. Crack tip displacement fields.

$$W = \int^{\varepsilon} \sigma_{ij} d\varepsilon_{ij} \quad ,$$

and I_n is a constant dependent on hardening index n. Terms $\hat{\varepsilon}_{ij}$ and $\hat{u}_i$ are functions of the polar coordinate θ and n. Since the crack growth is controlled largely by local phenomena at the crack tip, Shih[10] has hypothesized that the crack tip opening displacement (CTOD) δ_t should be a measure of the damage at the crack tip. He has shown that CTOD is related to J by

$$\delta_t = (\alpha\varepsilon_o)^{1/n} D_n \frac{J}{\sigma_o} \quad , \tag{11}$$

where D_n is a function of n. Tabulations of all these constants are available in Ref. 11.

Figure 4 compares typical normalized displacements u_2 and u_3 obtained from experimental results with those calculated by the HRR equations. Here δ_t is used for normalizing the displacements, and plate thickness h is used for the polar coordinate r. Experimental δ_t were measured by counting the total number of fringes between the lower and upper lips of the crack up to about 1 to 2 mm behind the visible crack tip position, where the crack lips are parallel. Plate thickness h is used to normalize r to bring out the 3-D effects around the crack tip, where plane

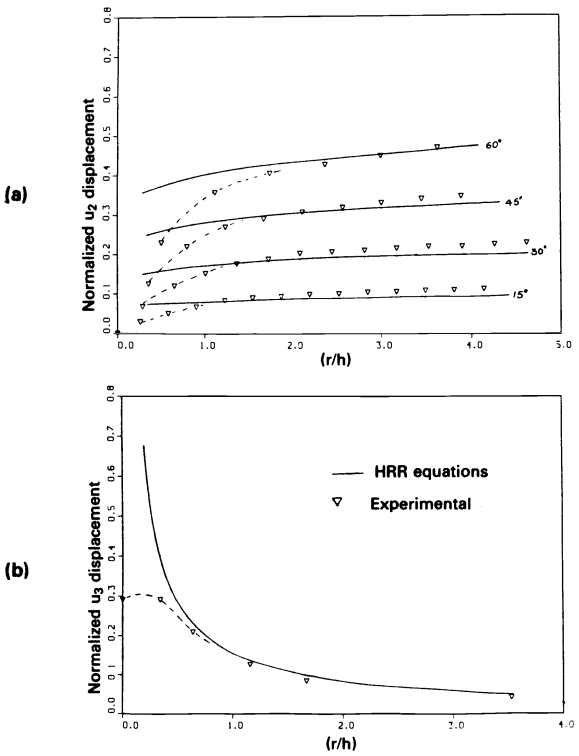

Fig. 4. Normalized displacements compared with plane stress HRR equations for (a) u_2 and (b) u_3.

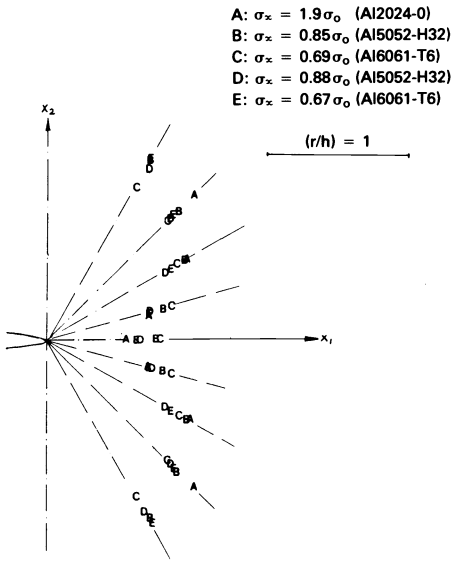

Fig. 5. Estimated 3-D zone around the crack tip.

stress assumptions break down owing to the finite plate thickness and crack tip blunting. In these figures, note that in the immediate vicinity of the crack tip there are marked deviations between experimental measurement and theory. The out-of-plane displacement u_3 is finite at the crack tip, unlike the theoretical prediction. To estimate the size of this region of dominant 3-D effects, we chose the boundary of the region to be at length r, where the difference between the HRR model and the experimental measurements of normalized displacements is ± 0.025 or more. Several experiments were done with three different materials, and results were plotted. In each case, the boundary of the 3-D effects was measured using the above criterion along discrete directions ahead of the crack tip. Figure 5 is a composite of all such measurements. Despite the experimental scatter, these data points seem to have a regular trend showing that the 3-D zone size is about 0.75h to 1.5h with direction dependence. This forms the "inner limit" of the HRR equations, beyond which the 2-D model seems to agree with the experimental observations.

Figures 6(a) and 6(b) are logarithmic plots of fringe order (equivalent to the opening displacement component u_2) versus r along different directions from the crack tip for two different materials. The solid line represents the slope $[1/(n+1)]$ of these experimental curves based on the HRR equations. Note that in each of these displacement plots there seems to be a region of constant slope (approximately that indicated by the solid lines) in a region where r ranges from about 5 mm to 13 to 15 mm. Outside this region, the slopes differ from those indicated by the HRR equations. In Fig. 6(c), the log of the opening strain ε_{22} is plotted against log (r) along $\theta = 0°$ (x_1 axis). The HRR field predicts a slope of $-n/(n+1)$ for the strain component, which is represented by the solid lines. The two types of triangles are the strain values calculated from the fringe patterns shown in the figures. Here again, there is a region of constant slope. In these logarithmic plots, the initial deviation in the slope, as explained earlier, is due to the 3-D effects near the crack tip. Deviation beyond r = 13 to 15 mm can be looked at as the "outer limit" of the HRR fields, where the singularity descriptions cease to dominate owing to the boundary effects of the specimen or the elastic field surrounding it.

The results obtained from the Al5052-H32 sample, for which the outer limit is at about 14 mm, are in fair agreement with those of Zehnder et al.[5] for a steel with similar hardening index ($n \approx 8.5$). Their investigations showed that the outer limit of the HRR field is at about a third of Irwin's plastic zone length factor r_p, given by

$$r_p = \frac{1}{\pi}\left(\frac{K}{\sigma_o}\right)^2 , \tag{12}$$

and the stress intensity factor K, given by

$$K = c\sigma_\infty\sqrt{\pi a'} , \tag{13}$$

where a′ is the corrected crack length to account for the deviations from small scale yielding assumptions,[12] c is a constant to account for geometrical effects of the specimen,[13] and σ_∞ is the far-field applied stress. Equations (12) and (13) give a value of $r_p/3$ equal to 12.5 mm, which is close to the value of 14 mm shown by plots 6(b) and 6(c) and where the curves begin to change slope. However, when similar calculations were done on the Al2024-0 results, $r_p/3$ turned out to be 53 mm, although the plots still show slope deviation at around 13 to 14 mm. This could be because Al2024-0 is a soft variety of aluminum and the applied far-field stress ($2.04\sigma_o$) had already resulted in net section yielding of the specimen. Thus, the above approach of estimating plastic zone length is unrealistic in this case. However, in both cases, for the same specimen geometry, the outer limit seems to occur at about 0.2b, where b is the uncracked ligament length of the sample.

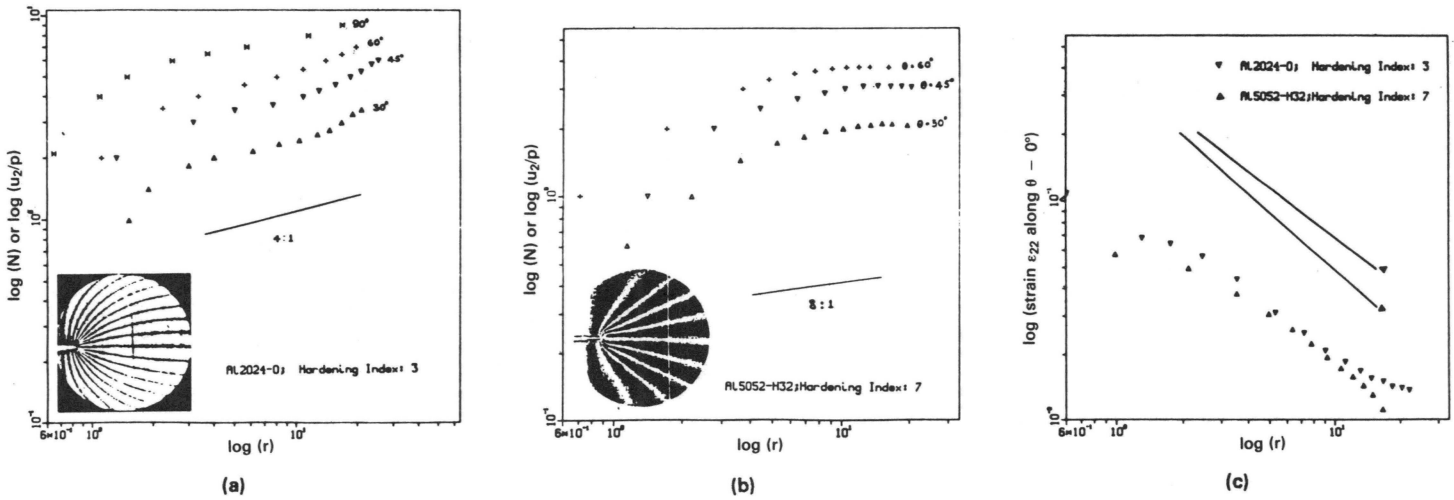

Fig. 6. Log (u_2) vs log (r) for (a) Al2024-0 and (b) Al5052-H32. (c) Log (ε_{22}) vs log (r).

5. CONCLUSIONS

Using a combined in-plane and out-of-plane moire method, we have been able to map out the complete displacement field around a plastically deformed crack tip. Comparison of the normalized displacements near the crack tip shows that there is a region around the crack tip where plane stress approximations do not hold owing to the strong 3-D effects. This zone is estimated to be from 0.75 to 1.5 times the thickness of the sheet with directional dependence. From the logarithmic plots of u_2 displacement and ε_{22} strain, we estimate the outer limit of plane stress HRR fields to be at about 13 or 14 mm. This measures out to about 0.2 times the uncracked ligament length.

6. ACKNOWLEDGMENTS

This work is supported by ONR Mechanics Division (Y. Rajapkse, Scientific Officer) Contract N0001482K0566 and NSF Solid and Geo-Mechanics Program (K. Thirumalai, Program Director) Grant MEA8403912.

7. REFERENCES

1. J. W. Hutchinson, "Singular behavior at the end of a tensile crack in a hardening material," J. Mech. Phys. Solids 16, 13–31 (1968).
2. J. R. Rice and G. F. Rosengren, "Plane strain deformation near a crack tip in a power law hardening material," J. Mech. Phys. Solids 16, 337–347 (1968).
3. A. J. Rosakis and K. Ravi Chandar, "On crack stress state: an experimental evaluation of three dimensional effects," Rept. SM84-2, Graduate Aeronautical Labs., California Institute of Technology (1984).
4. F. P. Chiang and T. V. Hareesh, "Three dimensional crack tip deformation: an experimental study and comparison to HRR field," Tech. Rept. 481, College of Engineering and Applied Sciences, SUNY at Stony Brook, (1986); Int. J. Fracture 36, 243–257 (1988).
5. A. T. Zehnder, A. J. Rosakis, and R. Narasimhan, "Measurement of the J integral with caustics: an experimental and numerical investigation," Rept. SM86-8, Graduate Aeronautical Labs., California Institute of Technology (1986).
6. B. S. J. Kang, A. S. Kobayashi, and D. Post, "Stable crack growth in aluminum tensile specimens," Tech. Rept., Univ. of Washington (1986).
7. A. S. Kobayashi and B. S. J. Kang, "Stable crack growth in aluminum tensile specimens," Exp. Mech. 27(3), 523–526 (1986).
8. C. F. Shih, "J-dominance under plane strain fully plastic conditions: the edge crack panel subjected to combined tension and bending," Int. J. Fracture 29, 73–84 (1985).
9. F. P. Chiang, "Techniques of optical spatial filtering applied to the processing of moiré fringe patterns," Exp. Mech. 6(11), 523–526 (1979).
10. C. F. Shih, "Relationship between the J-integral and the crack opening displacement for stationary and extending cracks," J. Mech. Phys. Solids 29, 305–326 (1981).
11. C. F. Shih, "Tables of HRR singular field quantities," Rept. MRL E-147, Materials Research Lab., Brown Univ. (1983).
12. M. F. Kanninen and C. H. Popelar, *Advanced Fracture Mechanics*, Oxford Engineering Science Series 15, Oxford University Press, New York (1985).
13. D. P. Rooke and D. J. Cartwrite, *Compedium of Stress Intensity Factors*, Her Majesty's Stationery Office, London (1975).

F. P. Chiang: Biography and photograph appear with the Guest Editorial on p. 595.

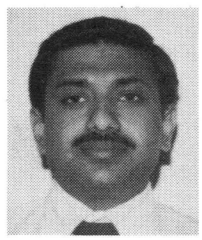

T. V. Hareesh graduated in 1980 from Bangalore University, India, with a bachelor's degree in mechanical engineering. In 1982 he received his master's degree in mechanical engineering from the Indian Institute of Science, after which he worked as a scientist in the Gas Turbine Research Establishment, Bangalore, India. Since 1983 he has been associated with the Laboratory for Experimental Mechanics Research, State University of New York at Stony Brook, where he received his Ph.D. degree in 1988. His research interests include optical and numerical methods for studying linear and nonlinear fracture of materials, NDE, material fatigue, and automation.

Bao-chen Liu graduated from the Department of Engineering Mechanics of Tsinghua University, Beijing, China, in 1959 (BS degree) and 1963 (Ph.D. degree). During 1963 to 1972, she worked on elastic-plastic analysis and experimental mechanics of shells and plates. Since 1975, she has been using optical methods in the field of fracture mechanics and engineering structure stress analysis. About 60 of her technical papers in these areas have been published. She is now an associate professor at Tsinghua University and a visiting professor in the Department of Mechanical Engineering, State University of New York at Stony Brook.

Shen Li received the BS degree from the Department of Mechanical Engineering at Beijing Institute of Posts & Communications, Beijing, China, in 1982. From 1982 to 1986, she was an assistant engineer for the Research Institute of Postal Science & Technology, Beijing, China. Now she is a graduate student in the Department of Mechanical Engineering, State University of New York at Stony Brook.